Supporting Information: Microfluidics-Based Selection of Red-Fluorescent Proteins with Decreased Rates of Photobleaching

Kevin M. Dean[a,b], Jennifer L. Lubbeck[b,c], Lloyd M. Davis[d,e], Chola K. Regmi[f], Prem P. Chapagain[f], Bernard S. Gerstman[f], Ralph Jimenez[b,c,*], and Amy E. Palmer[a,b,*]

[a]BioFrontiers Institute, University of Colorado, Boulder, CO, U.S.A.

[b]Department of Chemistry and Biochemistry, University of Colorado, Boulder, CO, U.S.A.

[c]JILA, NIST, and University of Colorado, Boulder, CO, U.S.A.

[d]Center for Laser Applications, University of Tennessee Space Institute, Tullahoma, TN, U.S.A.

[e]Department of Physics, University of Tennessee Knoxville, Knoxville, TN, U.S.A.

[f]Department of Physics, Florida International University, Miami, FL, U.S.A.

E-mail: amy.palmer@colorado.edu and rjimenez@jila.colorado.edu

Supporting Information includes:

Note S1 – Indirect versus direct measurement of the fluorescence quantum yield.

Fluorescence quantum yield is traditionally measured using a spectrophotometer and a fluorimeter. Here, the integrated fluorescence intensity as a function of optical density is measured for reference (*e.g.,* Rhodamine 101 and Cresyl Violet) and unknown (*e.g.,* mCherry and Kriek) fluorophores. Typically, 4-5 measurements are performed for each fluorophore, and the maximum optical density is kept below 0.1 per cm optical path length to avoid secondary absorption inner filter effects. The resulting data are subjected to a linear fit, which should have a y-intercept of 0 and unbiased error residuals. Using equation 1, the quantum yield of the unknown fluorophore (ϕ_x) can be calculated from the reference slope (m_{st}), reference refractive index (η_{st}), reference quantum yield (ϕ_{st}), unknown slope (m_x) and unknown refractive index (η_x).

$$\phi_X = \phi_{ST} \frac{m_x}{m_{ST}} \frac{\eta_X^2}{\eta_{ST}^2} \qquad (1)$$

Several experimental procedures can impact the reliability of this measurement. By using two reference fluorophores, as performed here, the error can be estimated by calculating the quantum yield of one reference with the other. To avoid inaccurate optical density measurements, increased integration periods and/or path lengths are used. Dual-beam operation minimizes lamp fluctuations, and accurate correction of the spectrophotometer baseline ensures that the measurement is not distorted spectrally (*e.g.,* from reflections or scatter). These factors are expected to be important when the optical density values are below 0.05, where small changes in the percent transmission significantly affect the measured optical density. Minimizing the duration of time between the measurement of the optical density and the integrated fluorescence intensity, as well as minimizing the number of sample transfers (*e.g.,* from one cuvette to another), decreases non-specific absorption and loss of sample, as well as evaporation of volatile solvents (ethanol for Rhodamine 101, and methanol for Cresyl Violet). Ideally, the fluorimeter PMT spectral response is well calibrated, and the reference fluorophores' emission is spectrally similar to the unknown. Furthermore, many reference fluorophores are vulnerable to environmental perturbations (*e.g.*, pH, concentration, temperature, ionic strength, etc.). Given these difficulties, using the fluorescence intensity-based approach, an error of ~10 % is typically observed after cross-calibration with the reference fluorophores.

In contrast, the time-correlated measurements of fluorescence lifetime performed here, by simply comparing mCherry to Kriek, avoid the day-to-day environmental complications associated with reference fluorophores. Determination of the optical density is unnecessary, thus eliminating inaccurate low optical density measurements and uncertainty arising from non-specific sample absorption and solvent evaporation. Measurements are performed away from the coverslip surface with confocal detection, thus avoiding surface-induced artifacts, and unlike PMTs, avalanche photodiodes are well suited for fluorescence detection beyond 600 nm. Experimental artifacts, including saturation of the time-correlated photon counting electronics, are well understood and easily avoided.[1] Perhaps most importantly, the lifetime measurements are based upon $>10^5$ photons sampled with 49 ps temporal resolution, and 100's of data points are used for the fit analysis (as opposed to ~5 for quantum yield). Using this methodology, we observed an exponential decay for mCherry of 1.639 +/- .002 ns and .875 +/- .002 ns for mCherry, and Kriek, respectively, providing a fit error of less than 0.2 %.

Therefore, because of the reduced sensitivity of the fluorescence-lifetime approach to experimental artifacts, this indirect measurement of the fluorescence efficiency gives more accurate values than the direct, fluorescence intensity-based approach.

Table S1. Mutations observed in Sort2.1 and Sort2.2.

RFP	16	66	143	161	163
mCherry	Val	Met	Trp	Ile	Gln
S2a			Ala	Leu	Ile
S2b			Cys	Val	Thre
Kriek			Ile	Met	Val
S2d	Ala	Gln	Met	Val	Leu
S2e	Ala	Gln	Ser	Val	Leu
S2f	Ala	Gln	Met	Val	Trp
S2g			Ala	Leu	Ile
S2h			Ser	Val	Leu
S2i			Ser	Val	Leu
S2j			Ala	Leu	Ile
S2k		Gln	Ala	Leu	Ile
S2l			Ser	Val	Leu
S2m			Ala	Leu	Ile
S2n			Ser	Val	Leu
S2o			Ala		
S2p			Ala	Leu	Ile
S2q			Ala	Leu	Ile
S2r			Ala	Leu	Ile
S2s			Ala	Leu	Ile
S2t			Ala	Leu	Ile

Mutants with Val16Ala mutations also had an unintended mutation, His17Arg, likely arising from an error in primer synthesis. mCherry was identified in 12 of the 32 clones sequenced.

Table S2. Spectral Properties of Kriek Mutants.

RFP	λ_{abs} (nm)	λ_{ex} (nm)	λ_{em} □□□□
mCherry W143I	583	583	611
mCherry I161M	588	592	617
mCherry Q163V	585	586	614
mCherry W143I I161M	589	592	618
mCherry W143I Q163V	587	588	618
mCherry I161M Q163V	588	590	612

Individual mutations are listed, and reported values are the absorption and emission maxima at pH=7.4.

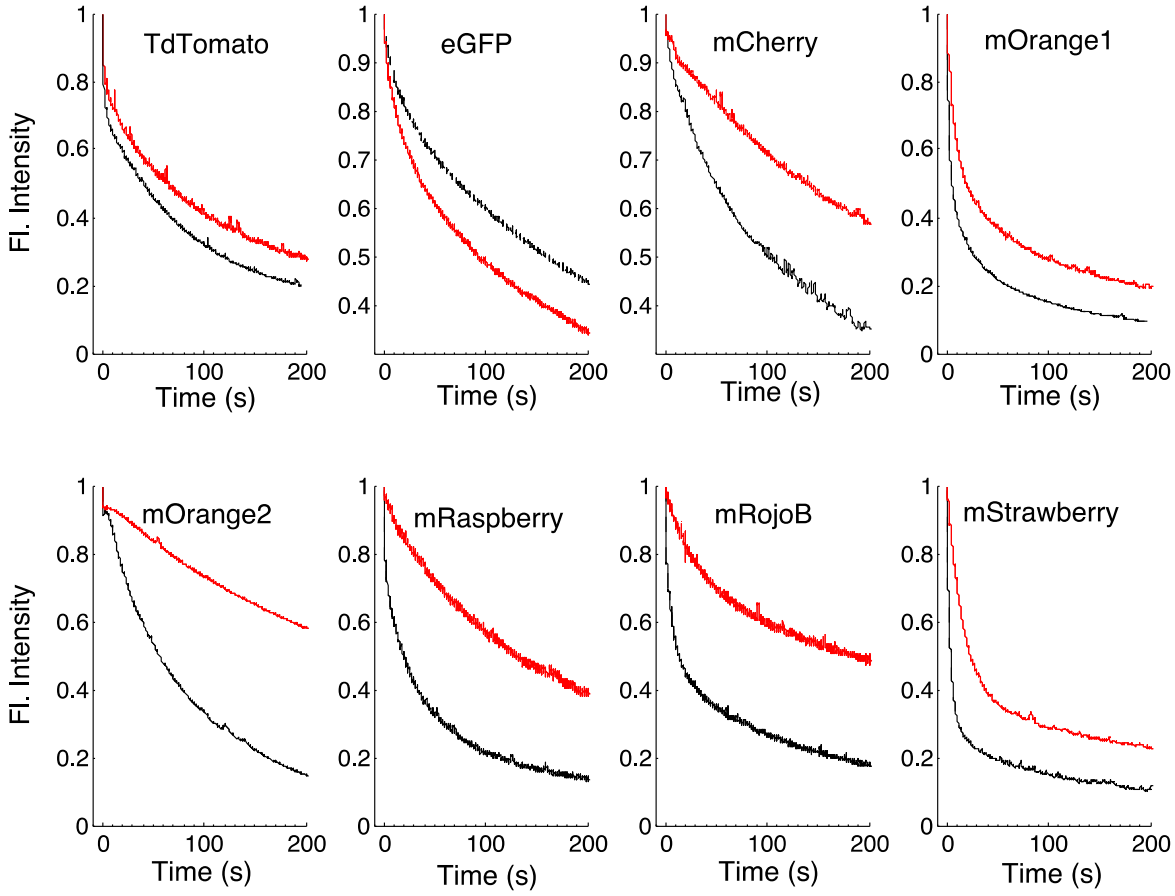

Figure S1. Qualitative Aerobic and Anaerobic Measurements of FP-Expressing E. coli. Red - Anaerobic, Black - Aerobic. Measurements were performed in a widefield format on Poly-l-Lysine immobilized E. coli before and after purging the environment with N_2 for 30 minutes. Measurements are considered qualitative since the absolute $^3O_2$ concentration within solution and the bacteria was not measured. FPs exhibited varying levels of oxygen sensitivity (e.g., TdTomato vs mOrange2), and eGFP appeared to photobleach more rapidly in the presence of $^3O_2$. Accelerated photobleaching in the absence of $^3O_2$ has been observed elsewhere, and is attributed to decreased triplet-state quenching.[2]

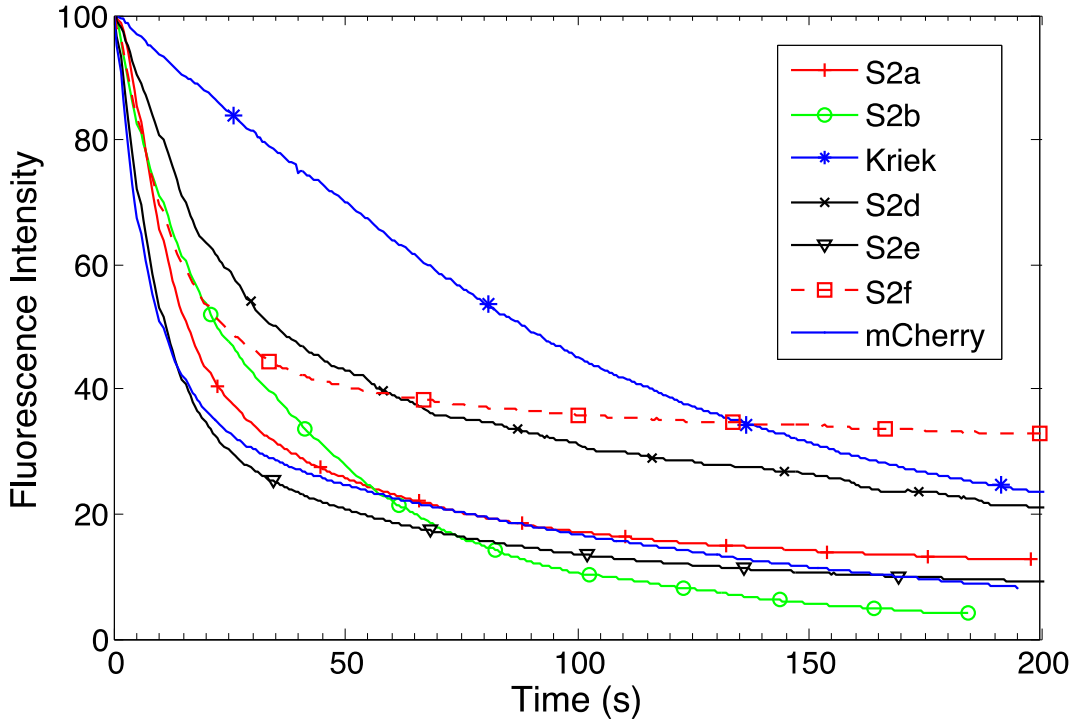

Figure S2. Photobleaching Decay of Kriek Mutants and mCherry in Immiscible Octanol Droplets. Purified protein diluted 1:10 with octanol, briefly vortexed, sandwiched between two coverslips, and subjected to laser-scanning confocal photobleaching with 6 mW of a 561 nm excitation laser. The resulting decay for multiple droplets were corrected for image background, and fit to a biexponential decay. Some FPs displayed a fast decrease followed by a slower photobleaching decay (e.g., K2f), whereas others photobleached more gradually throughout (e.g., K2c and K2d).

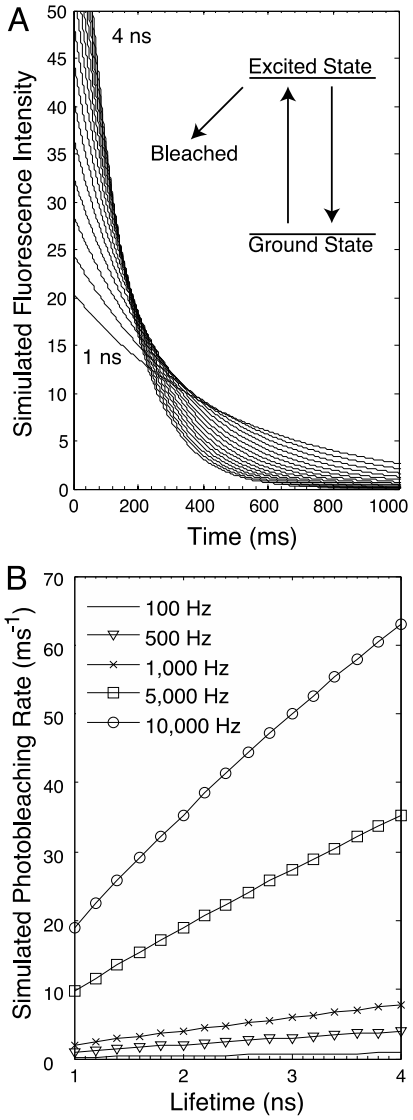

Figure S3. Numerical Simulations of Photobleaching with a Two-State System. (A) Numerical simulations of a two-state system at 2 kW/cm^2 excitation intensity. For each photobleaching rate, the fluorescence lifetime was varied between 1 nanosecond (bottom curve) and 4 nanoseconds (top curve) in 0.2 nanosecond steps (intermediate curves). The resulting decay was fit to determine the apparent rate of photobleaching, and a single exponential decay accurately described these data. (B) The simulated photobleaching rate determined from fitting the decays in A, and the rate of photobleaching was found to increase linearly with the fluorescence lifetime, with deviations from linearity observed at high photobleaching rates (*e.g.,* > 10,000 Hz).

Supporting References

1. A. W. Castleman, W. Becker, J. P. Toennies and W. Zinth, 2005, **81**.
2. C. Eggeling, A. Volkmer and C. A. M. Seidel, *ChemPhysChem*, 2005, **6**, 791-804.